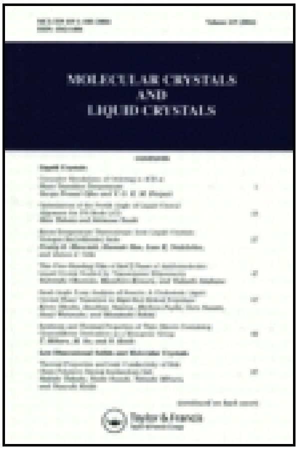

Molecular Crystals and Liquid Crystals

Publication details, including instructions for authors and subscription information:
http://www.tandfonline.com/loi/gmcl20

Numerical Modeling of Tunable Liquid-Crystal-Polymer-Network Lens

Svitlana L. Subota [a] , Victor Yu. Reshetnyak [a] , Svitlana P. Pavliuchenko [a] & Timothy J. Sluckin [b]

[a] Physics Faculty, Kyiv National Taras Shevchenko University, Kyiv, Ukraine

[b] School of Mathematics, University of Southampton, Highfield, Southampton, United Kingdom

Version of record first published: 05 Apr 2011

To cite this article: Svitlana L. Subota, Victor Yu. Reshetnyak, Svitlana P. Pavliuchenko & Timothy J. Sluckin (2008): Numerical Modeling of Tunable Liquid-Crystal-Polymer-Network Lens, Molecular Crystals and Liquid Crystals, 489:1, 40/[366]-53/[379]

To link to this article: http://dx.doi.org/10.1080/15421400802219866

Mol. Cryst. Liq. Cryst., Vol. 489, pp. 40/[366]–53/[379], 2008

ISSN: 1542-1406 print/1563-5287 online
DOI: 10.1080/15421400802219866

Numerical Modeling of Tunable Liquid-Crystal-Polymer-Network Lens

Svitlana L. Subota[1], **Victor Yu. Reshetnyak**[1],
Svitlana P. Pavliuchenko[1], **and Timothy J. Sluckin**[2]
[1]Physics Faculty, Kyiv National Taras Shevchenko University, Kyiv, Ukraine
[2]School of Mathematics, University of Southampton, Highfield, Southampton, United Kingdom

A gradient polymer stabilized liquid crystal (G-PSLC) structure has recently been proposed for a tunable-focus lens application. A homogeneously-oriented nematic liquid crystal (NLC) cell, doped by a few percent of photopolymerizable monomer, is initially illuminated by a laser beam with a Gaussian spatial intensity distribution. This induces a spatially inhomogeneous polymer network in the cell. The electro-optical response of this system to a uniform electric field exhibits an inhomogeneous circularly symmetric pattern. The radial distribution of the effective refractive index possesses a maximum in the center of the beam. This cell acts as a positive focal length lens on the extraordinary polarized light component passing through it. The profile of the refractive index in the plane of the cell can be changed by varying the voltage across the cell. Thus the focal length of the lens changes with voltage. Here we present a numerical approach to our earlier theoretical model. The model describes the dependence of the focal length of the G-PSLC lens on applied voltage. The new feature of the model is that we have used several trial functions for the form of the polymer profile. The director profile in the cell was determined as a function of voltage. The model qualitatively agrees with the experimental data. The results can be applied to develop G-PSLC lenses with no moving parts and permit electro-optical zooming.

Keywords: adaptive optics; polymer-stabilized liquid crystal; tunable focus liquid crystal lens; variable focus

We acknowledge NATO grant CBP.NUKR.CLG.981968, which supported visits by VYR and SLS to Southampton, where some of this work was carried out. We are also grateful to the Royal Society (UK) for support in the early phase of this project, and who supported visits of SLS and VYR to Southampton and TJS to Kyiv. We are also grateful to Tigran Galstian (Quebec) and Giancarlo Abbate (Napoli) for fruitful discussions.

Address correspondence to Svitlana L. Subota, Physics Faculty, Kyiv National Taras Shevchenko University, Prosp. Glushkova 2, build. 1, Kyiv, 03680, Ukraine. E-mail: subota@univ.kiev.ua

1. INTRODUCTION

Liquid crystals are used in a variety of optical devices and in many applications, such as displays, deflectors, modulators and flaw detectors. In recent years there has been much interest in active optical elements, such as lenses with variable focal length [1–10]. Liquid crystals are anisotropic media. The phase lag of the extraordinary wave with respect to the ordinary wave depends on the angle between the light propagation direction and the easy axes. Most tunable lenses depend on director reorientation, leading to modified transmission properties for extraordinary waves.

The key piece of physics is that the phase lag of the extraordinary wave can be dependent on position in the plane of the cell. If liquid crystal molecular reorientation changes with lateral position in the cell, then the phase lag will not be constant within the cell plane. If the functional dependence is suitable, the cell can acts as a lens. One suitable condition occurs when the director reorientation characteristics are radial symmetric. The lens is tunable because the degree of phase shift can be altered by reorienting the liquid crystal using electric or magnetic fields.

A number of possible designs for liquid crystal cells are now available. They differ in the methods used to create the inhomogeneous director distribution. For example, the inhomogeneous electric fields inside the cell can be created by using electrodes with holes [1–4] or by non-planar electrodes [5,6]. Such fields induce laterally inhomogeneous director reorientation and refractive index. However, this cell configuration usually requires relatively high voltages and responds only slowly on switch-on and switch-off. This design is suitable for use as a microlens.

An alternative lens construction design employs Fresnel zones. Monomers are polymerized by laser light, but during polymerization process a photomask is introduced by odd-even Fresnel zones. The cell involves a laterally inhomogeneous polymer concentration [7]. In an electrical field the refractive index is also laterally inhomogeneous. The resulting lens has working voltage range of 4–10 V.

Another subsequent lens design is also based on Fresnel zones. Several ring electrodes on a cell wall form Fresnel zones [8]. The voltage across these electrodes changes slowly as a function of position. This scheme has been proposed as a design for optical spectacles. Advantages of the scheme are that only low voltages are required, and optical strengths of several dioptres are in an appropriate range, but a disadvantage is that the resulting product is quite bulky.

In this paper we consider an alternative lens design. This is the gradient polymer stabilized liquid crystal (G-PSLC) tunable lens [9,10]. A mixture of planar oriented nematic liquid crystal (NLC) and a few percent of photopolymerizable monomer is illuminated by laser beam with a Gaussian spatial intensity distribution. This treatment induces a spatially inhomogeneous polymer network. This geometry preserves director reorientation when a constant electric field is applied. The test light beam is refracted by the inhomogeneous director. Thus a liquid crystal lens is created. Since the director reorientation angle depends on external field, the focal length can also be tuned by changing the external voltage.

The advantages of this lens are low control voltage, large size and simple production. In addition, only constant field is required, as opposed to subtly changing field across field of view. Typical lens sizes are ~2–3 mm, and focal lengths in the range 0.5–4 m.

The purpose of this paper is to construct the basic theoretical framework within which the behavior of this class of lenses can be understood. A preliminary report of this work has appeared in MCLC [11]. In this article we present further improvements of this problem, involving numerical solutions.

The plan of this paper is as follows. In §2 we describe the model problem. In §3 we discuss reorientation of the director in a constant electric field in the presence of the induced polymer network. In §4 we examine the characteristics of the liquid crystal lens. Finally in §5 we draw some brief conclusions.

2. MODEL

Let us consider a NLC and monomer mixture placed in a cell with thickness L with planar and uniform boundary conditions at each wall. We assume there is strong director anchoring at the cell walls. The cell is illuminated by UV laser beam:

$$I = I_0 \exp(-\alpha\rho^2), \tag{1}$$

where we denote $\alpha = 1/2\varpi^2$, and where ϖ is a half-width of the Gaussian beam.

Polymerization then occurs, and after some time the polymerisation process stabilizes. The resulting stationary polymer concentration depends on radial coordinate. We assume that there is no significant light absorption through the cell during polymerization process, as a result of which the polymer concentration does not depend on distance from the cell walls. The polymer retains a memory of the initial planar

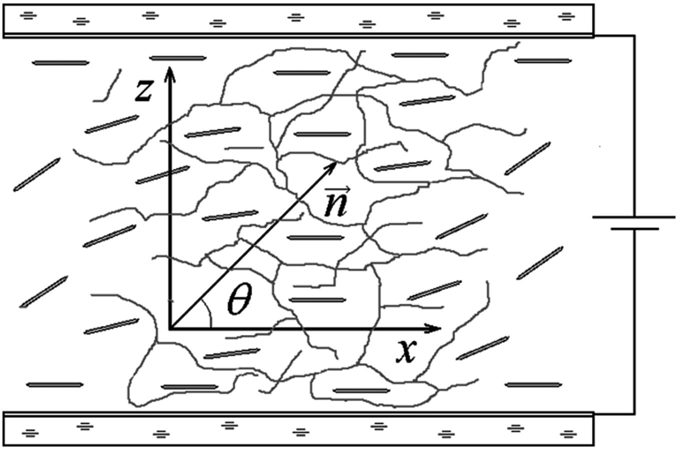

FIGURE 1 LC cell geometry. See text for explanation.

alignment. The anchoring between the liquid crystal director and the locally quenched polymer orientation then differentially prevents director reorientation in an applied voltage.

The geometry of the lens cell is shown in Figure 1. Axis Ox is directed along the initial director direction. Oz is perpendicular to the cell walls, and an electric field is $\vec{E} = (0, 0, E(z))$ is applied in this direction. The field reorients the director, and it plausible to assume that the director remains in the xz-plane only. The refractive index profile varies as the field is applied. The profile induces lens-like behavior, the focal length of which is also field-dependent.

3. DIRECTOR REORIENTATION

In order to investigate the director reorientation in electrical field we numerically minimize the free energy:

$$F = \frac{1}{2}\left[K_{11}\int(\nabla.\mathbf{n})^2 dV + K_{22}\int(\mathbf{n}\cdot\nabla\times\mathbf{n})^2 dV + K_{33}\int(\mathbf{n}\times\nabla\times\mathbf{n})^2 dV\right] - \frac{W}{2}\int N_p(\mathbf{r})(\mathbf{n}\cdot\mathbf{e})^2 dV - \frac{1}{2}\int(\mathbf{D}\cdot\mathbf{E})^2 dV. \quad (2)$$

The first three terms in (2) are the usual elastic contribution to the LC total free energy. In the final term, **D** is the electric displacement vector, which depends on **E** through the director **n**; this term is essentially the usual anisotropy energy of a nematic.

The key term for this theory is the fourth term in (2). Here N_p is the density of the polymer network, W is the anchoring energy between polymer and liquid crystal orientations, and $\mathbf{e}$ is an unperturbed director orientation. The effect of this term is the existence of an extra torque on the liquid crystal due to the presence of the polymer network created by the non-uniform UV beam. An investigation of the spatial dependence $N_p(\mathbf{r})$ is a rather complicated task and requires a separate study. We need to solve the set of rate equations [11–13]. The main difficulty is to find rate constants, which can depend on temperature, solution concentration and stage of polymerization. So in this paper we consider different trial forms for the polymer profile.

Although neither N_p nor W are known experimentally, it is convenient to introduce a new parameter $w = WN_p$, the local effective bulk anchoring energy per unit volume. The magnitude of the parameter w can be directly determined from a measurement of the Frederiks transition threshold shift in a pure cell illuminated by a uniform UV beam.

By radial symmetry, the director field is given by

$$\mathrm{n} = (\cos\theta(\rho,z), 0, \sin\theta(\rho,z)) \tag{3}$$

The Maxwell equations for the LC cell in electric field are:

$$\begin{cases} \nabla\,.\,\mathbf{D} = \frac{\partial \mathbf{D}_z}{\partial \mathbf{z}} + \frac{1}{\rho}\frac{\partial(\rho \mathbf{D}_\rho)}{\partial \rho} = 0 \\ \nabla \times \mathbf{E} = 0 \end{cases} \tag{4}$$

The electric field in the z direction varies on a length scale $L \sim 10\mu$. By contrast, the scale of the inhomogeneity in the cell plane $\sim 1\,\mathrm{mm}$. The $\partial/\partial\rho$ derivatives in Eq. (4) can therefore be neglected in comparison with $\partial/\partial z$ derivatives. The rather complicated partial differential equations reduce to an easily solved set of ordinary differential equations in which the radial coordinate ρ can be regarded as a parameter.

Equation (4a) thus yields to good approximation $D_z = F(\rho)$. Solving Eq. (4b) yields $\mathbf{E} = (0, 0, E(\rho,z))$. Noting the standard result $D_z = \varepsilon_{zz}E_z = (\varepsilon_\perp + \varepsilon_a \sin^2\theta(z))E_z = \varepsilon_\perp E_0 = F(\rho)$ we derive the following relation for the voltage U across the nematic cell:

$$U = \int_0^L E dz = D_z \int_0^L (\varepsilon_\perp + \varepsilon_a \sin^2\theta(z,\rho))^{-1} dz. \tag{5}$$

The free energy functional (2) per unit area can now be simplified:

$$F = \frac{1}{2}K\int [(\theta'_z)^2 + (\theta'_\rho)^2] dV - \frac{W}{2}\int N_p(\mathbf{r})\cos^2\theta dV \\ - \frac{1}{2}\int D_z^2(\varepsilon_\perp + \varepsilon_a \sin^2\theta)^{-1} dV. \tag{6}$$

For simplicity we suppose the one elastic constant approximation: $K_1 = K_2 = K_3 = K$. By minimizing the functional (6) we obtain the following Euler-Lagrange equation in terms of D_z:

$$K\frac{\partial^2\theta}{\partial z^2} - w(\rho)\sin\theta\cos\theta + D_z^2\frac{\varepsilon_a\sin\theta\cos\theta}{(\varepsilon_\perp + \varepsilon_a\sin^2\theta)^2} = 0. \tag{7}$$

In this equation we neglect the $\partial/\partial\rho$ derivatives as they are small comparing to $\partial/\partial z$ derivatives; this assumption has been confirmed by numerical calculation in particular cases. We also assume strong anchoring at the cell walls:

$$\theta|_{z=0} = \theta|_{z=L} = 0. \tag{8}$$

It is convenient to re-write Eq. (7) in non-dimensional parameters:

$$\theta''_{uu} - \tilde{w}(v)\sin\theta\cos\theta + d_z^2\frac{\sin\theta\cos\theta}{\left(1 + \frac{\varepsilon_a}{\varepsilon_\perp}\sin^2\theta\right)^2} = 0, \tag{9}$$

where $u = z/L$, $v = \rho/L$, $\tilde{w}(v) = w(v)L^2/K$ and $d_z^2 = D_z^2L^2\varepsilon_a/K(\varepsilon_\perp)^2$. The boundary conditions for this Eq. (9) take the form:

$$\theta(\nu,0) = \theta(\nu,1) = \theta'(0,u) = \theta'(\infty,u) = 0 \tag{10}$$

In the absence of polymer diffusion during the polymerization process, we may expect the UV light intensity profile and the polymer profile to be of the same form. We thus use a Gaussian as an initial trial polymer concentration profile:

$$\tilde{w}(v) = w_0\exp(-\beta L^2v^2). \tag{11}$$

Here we have two parameters. In our previous theoretical work [11] we estimated a value of $w_0 \approx 11$ using experimental data [10]. Here we will study how the lens characteristics depend on the non-dimensionalized LC- polymer anchoring interaction w_0. The parameter β governs the width of the polymer profile. As discussed in [11], we investigate the range $0.5\alpha \le \beta \le 1.5\alpha$.

We have solved Eq. (9) with boundary conditions (10) numerically, using a finite element method [14]. Our model calculations use a cell thickness $L = 10\,\mathrm{M}$ and liquid crystal parameters for the liquid crystal E7 [15]. The principal components of the low frequency dielectric tensor are given by $\varepsilon_{||} = 19, \varepsilon_\perp = 5.2$, the principal refractive indices are given by $\sqrt{\tilde{\varepsilon}_{||}} = n_e = 1.738$, $\sqrt{\tilde{\varepsilon}_\perp} = n_o = 1.518$, and elastic constant is given by $K \approx 10^{-11}N$.

4. RESULTS

4.1. Director Reorientation

The director deviation profile for different values of applied voltage $V = U/U_0^{th}$ is shown in Figure 2. The scaling parameter U_0^{th} is the Frederiks threshold voltage for pure LC. The effective Frederiks transition is a local radially-dependent quantity. It is maximal where the intensity of polymerizing beam intensity is maximal in the center of the UV beam.

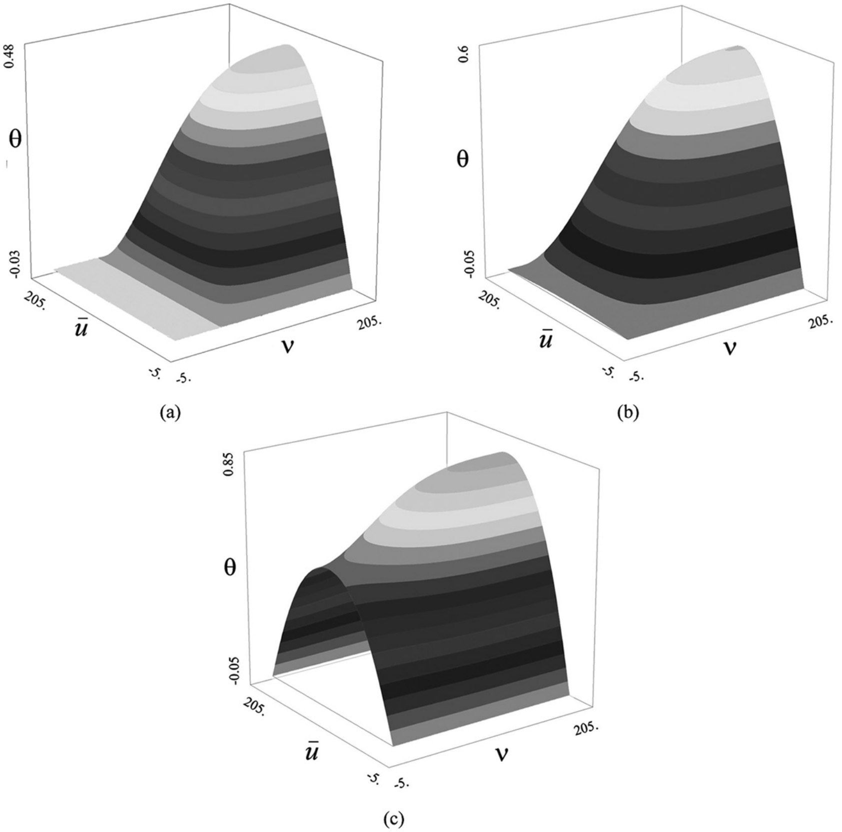

FIGURE 2 Inhomogeneous director reorientation angle at dimensionless voltage (where $w_0 = 11$, $\beta = 1.5 \cdot 10^6 \mathrm{m}^{-2}$) (a) V = 1.3, (b) V = 1.45, (c) V = 2.0. ν corresponds to radial coordinate and $\bar{u} = zb/L$ is a coordinate in the test ray transmission direction, here $b = 200$ is a scale coefficient, which was introduced for better visualization.

An alternative parameterization of the polymer concentration profile is a parabolic form:

$$\begin{cases} \tilde{w}(v) = w_0(1 - v^2/r_0^2), & v \le r_0 \\ 0, & v > r_0 \end{cases} \tag{12}$$

Director reorientation profiles have been calculated for the set of parameters r_0 and w_0. Some examples of director reorientation angle in this case are shown on Figure 3. We find that in all cases the director orientation profiles (shown in Fig. 3) follow very closely the polymer network profiles (shown in Fig. 2).

4.2. Focal Length

We now discuss the optical properties of the complete inhomogeneous liquid crystal slab. We may suppose that light passing through the system is insufficiently intense to perturb the polymer network further. In a conventional convex lens geometry requires that the component of a test beam passing through the center of the lens is subject to a larger phase lag than is the component passing near the edge of the lens. In the system under consideration, a polarized test beam is similarly subject to a differential phase lag, although in this case the differential phase lag is induced not by geometry but by spatial modulation of the optical properties. Thus we may say that an optical lens is created in the cell. Furthermore, because the differential phase lag is itself a function of external voltage, the lens properties are electrically controllable.

We confine our interest to the extraordinary wave. The ordinary wave is subject to a phase lag. However, this phase lag is uniform across the cell, and no lens is therefore induced. The phase lag profile of the extraordinary wave is given by the following formula [16]:

$$\varphi(\rho) = \frac{2\pi}{\lambda} \int_0^L n(\rho, z')dz', \tag{13}$$

where

$$n(\rho, z') = \frac{\sqrt{\tilde{\varepsilon}_{||}\tilde{\varepsilon}_{\perp}}}{(\tilde{\varepsilon}_{||}\cos^2\psi + \tilde{\varepsilon}_{\perp}\sin^2\psi)^{1/2}} \tag{14}$$

is the refractive index for the extraordinary beam propagating in the LC cell, $\psi(\rho, z')$ is the angle between the director (or equivalently the optical axis) at (ρ, z') and the light beam wave vector, $\hat{\tilde{\varepsilon}}$ is the dielectric tensor at optical frequency. In our case, $\psi = \pi/2 - \theta$, where θ is the director deviation calculated in §3.

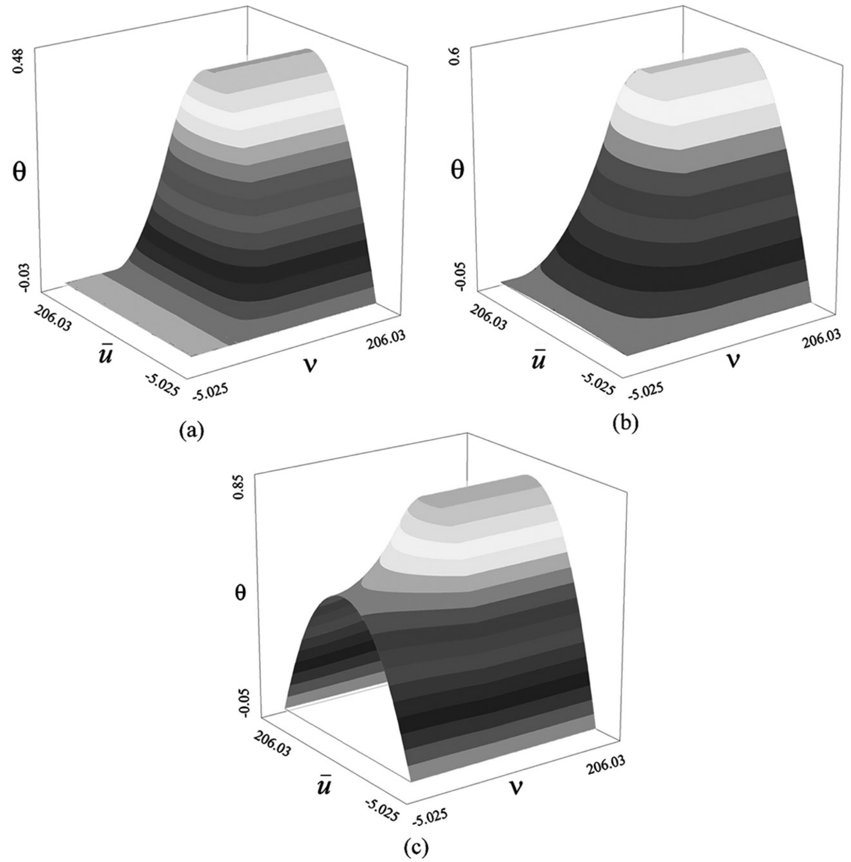

FIGURE 3 Inhomogeneous director reorientation angle at dimensionless voltage (where $w_0 = 11$, $r_0 = 90$) (a) V = 1.3, (b) V = 1.45, (c) V = 2.0. ν and $\bar{u}$ have the same meanings as in the previous figure.

To determine the effective focal length of the lens we fit (13) to a parabola [17]:

$$\varphi(\rho) = a - \frac{k\rho^2}{2f}, \tag{15}$$

where $a = \varphi(0)$ is the phase shift at the center of the initial UV beam and k is the wave vector of the test beam. Then the focal length is given by the best estimator to f.

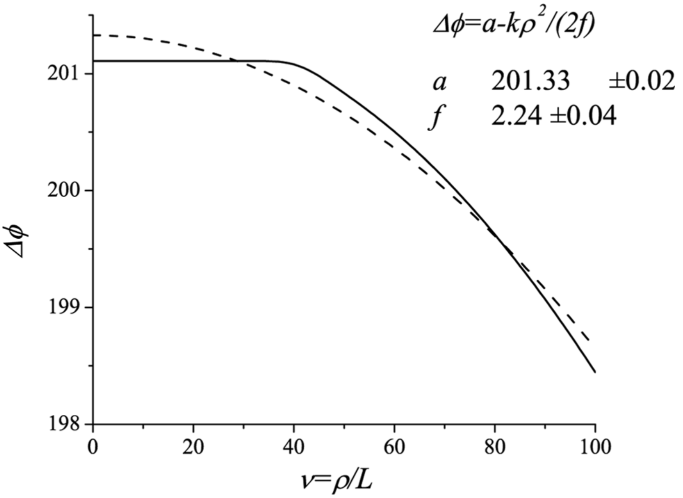

FIGURE 4 Approximation (dash line) of phase lag (solid line) at $V = 1.4$, $w_0 = 11$, $\beta = 1.5 \cdot 10^6 m^{-2}$.

If the applied voltage is below the Frederiks threshold value in the middle of the cell the fit is poor, as can be seen in Figure 4. In this case, the central part of the cell does not act as a lens, but on the other hand the sides of the cell do nevertheless focus a part of the light beam.

If the fit (15) is poor, then the lens will be subject to significant spherical aberration. This effect can be mitigated by inserting a shield with circular aperture with radius ρ_0 after the cell. The fit (15) is better if only a small region around $\rho < \rho_0$ is included. Under these circumstances, a sensible estimator for f is given by

$$f = \frac{k\rho_0^2}{2(\varphi(0) - \varphi(\rho_0))}, \tag{16}$$

For example, in their experiments Presnyakov *et al*. [9] used a test light beam with diameter $2\rho = 0.7\,\text{mm}$. In our estimation of the effective f, we have used values of ρ_0 of 0.25 and 0.5 mm, which are in the experimental range.

In Figures 5 and 6 we plot the dependence of the focal length on the applied voltage for different sets of parameters. We find, as we might expect, that all other things being equal, small lenses provide the highest lens power. This result seems robust. In addition, for the forms

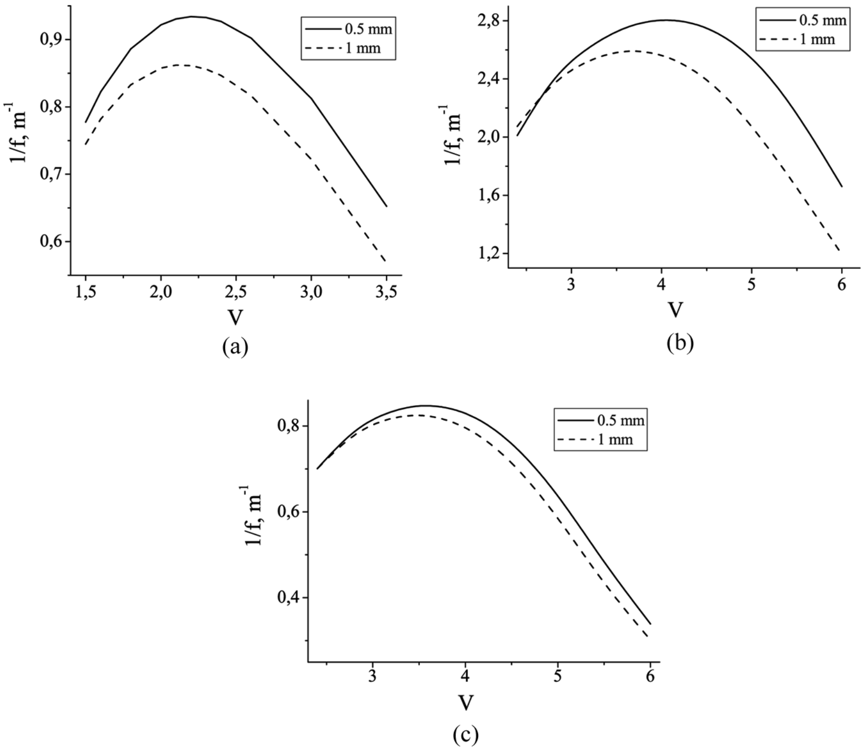

(a) (b) (c)

FIGURE 5 Dependence of lens power on applied dimensionless voltage, assuming a Gaussian polymer network profile (11) in director reorientation calculation: (a) $w_0 = 11$, $\beta = 1.5 \cdot 10^6 \mathrm{m}^{-2}$; (b) $w_0 = 44$, $\beta = 2.26 \cdot 10^6 \mathrm{m}^{-2}$; (c) $w_0 = 33$, $\beta = 0.76 \cdot 10^6 \mathrm{m}^{-2}$. Lens aperture diameters: (i) $2\rho_0 = 0.5\,\mathrm{mm}$ and (ii) $2\rho_0 = 1\,\mathrm{mm}$.

of lens we consider, the effective lens power is greater if a small aperture is inserted. Equivalently, the spherical aberration acts to reduce the effective lens power (and increase the focal length). The robustness of this result is not at this stage clear.

The w_0 dependence of (a) the maximal lens power f_m and (b) the voltage V_m at which this maximal lens power is attained, are shown in Figure 7. These plots assume the Gaussian polymer profile (11). For the parabolic polymer profile (12) analogous results can be derived. The key result is that if the interaction between the liquid crystal and the polymer is increased, so (unsurprisingly) does the maximal optical strength of the lens. However, in order to achieve this maximal strength, the operating voltage must also increase.

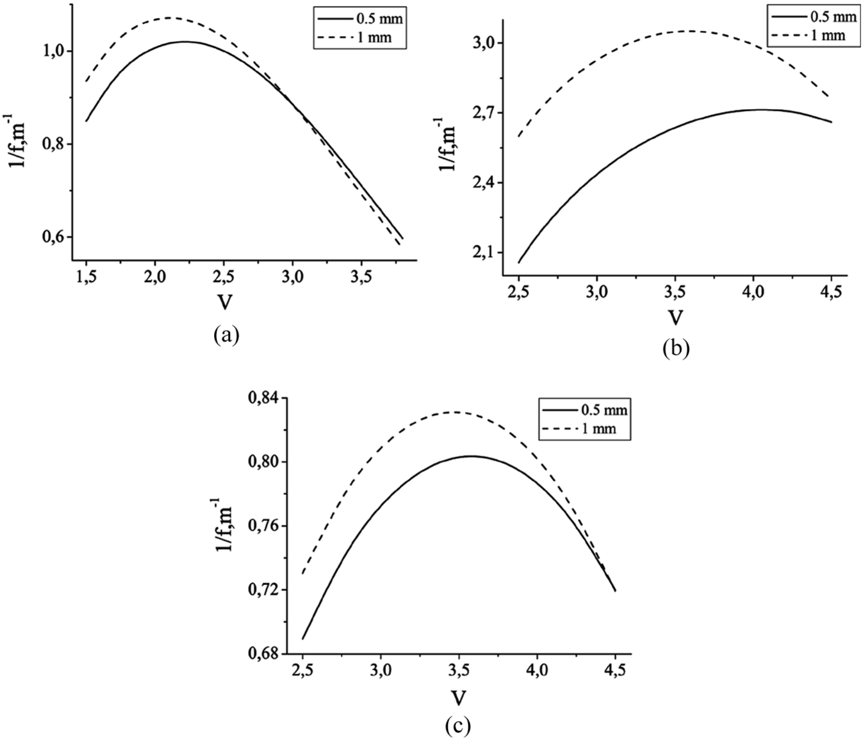

FIGURE 6 Parabolic polymer network profile (12) in director reorientation calculation; focal length dependence on the applied dimensionless voltage: (a) $w_0 = 11$, $r_0 = 80$; (b) $w_0 = 44$, $r_0 = 70$, (c) $w_0 = 33$, $r_0 = 120$. Lens aperture diameters as in previous figure.

5. CONCLUSIONS

G-PSLC lenses have no moving parts and permit electro-optical zooming, and therefore have significant potential for applications in a variety of electro-photonic devices. We have presented a theoretical model describing the dependence of the focal length of these lenses on applied voltage. By minimizing the total free energy functional for the liquid crystal in the complete cell, we find the director profile subject to an externally applied electric field. The polymer network creates an additional torque on the LC director. Gaussian and parabolic forms for the polymer network profile have been investigated. The polymer enables LC to preserve its planar orientation, despite an applied voltage which would otherwise be above the threshold voltage. The result is an inhomogeneous refractive index. It is this tunable inhomogeneous

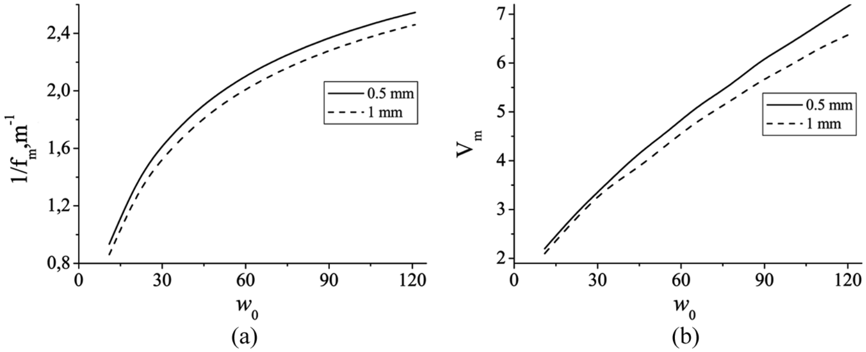

FIGURE 7 Gaussian polymer network profile (11), $\beta = 1.5 \cdot 10^6 \mathrm{m}^{-2}$ with aperture sizes 0.5 and 1 mm. w_0 dependence of: a) maximal lens power f_m; b) voltage V_m, at which maximal lens power is attained.

refractive index which gives rise to the lens effect. The focal length of this LC-lens decreases with increasing voltage and then increases. Increasing the interaction between the liquid crystal and the polymer network increases the optical strength of the lens, but at the same time also significantly increases the operating voltage. All other things being equal, lenses with a restricted lateral dimension are more powerful than those extending further in the cell plane. Our results enable improved quantitative understanding of the G-PSLC lenses and thus enable an improved design process for the device parameters. In future work, we shall consider in more detail specific lens parameters, in particular concentrating on chromatic and spherical aberration effects.

REFERENCES

[1] Naumov, F., Love, G. D., Loktev, Yu, M., & Vladimirov, F. L. (1999). *Optics Express*, *4*, 344.
[2] Nose, T., Masuda, S., & Sato, S. (1992). *Jpn. J. Appl. Phys.*, *31*, 1643.
[3] Ye, M. & Sato, S. (2002). *Jpn. J. Appl. Phys.*, *41*, L 571.
[4] Pishnyak, O., Sato, S., & Lavrentovich, O. D. (2006). *Appl. Opt.*, *45*, 4576.
[5] Wang, B., Ye, M., Honma, M., Nose, T., & Sato, S. (2002). *Jpn. J. Appl. Phys.*, *41*, L 1232.
[6] Ren, H., Fan, Y.-H., Gauza, S., & Wu, S.-T. (2004). *Appl. Phys. Lett.*, *84*, 4789.
[7] Fan, Y.-H., Ren, H., & Wu, S.-T. (2003). *Optics Express*, *11*, 3080.
[8] Li, G., Mathine, D. L., Valley, P., Äyräs, P., Haddock, J. N., Giridhar, M. S., Williby, G., Schwiegerling, J., Meredith, G. R., Kippelen, B., Honkanen, S., & Peyghambarian, N. (2006). *Proc. Nat. Acad. Sci. USA*, *103*, 6100.
[9] Presnyakov, V. V., Asatryan, K. E., Galstian, T. V., & Tork, A. (2002). *Opt. Express*, *10*, 865.

[10] Presnyakov, V. & Galstian, T. V. (2005). *J. App. Phys.*, *97*, 103101.

[11] Reshetnyak, V. Yu., Subota, S. L., & Galstian, T. V. (2006). *Mol. Cryst. Liq. Cryst.*, *454*, 187/[589]–200/[602].

[12] see e.g. Atkins, P. W. (1988). *Physical Chemistry*, Oxford University Press: Oxford, Ch. 29, 713.

[13] Caputo, R., Sukhov, A. V., Tabiryan, N. V., Umeton, C., & Ushakov, R. F. (2001). *Chem. Phys.*, *271*, 323.

[14] Gallagher, R. H. (1975). *Finite Method Analysis*, Prentice-Hall: New Jersey.

[15] Drzaic, P. S. & Muller, A. (1989). *Liq. Cryst.*, *5*, 1467.

[16] Goodman, D. S. (1995). Geometric optics. In: *Handbook of Optics*, Bass, M. (Ed.), McGraw-Hill: New York, Ch. 1, I.22.

[17] Goodman, J. W. (2002). *Introduction to Fourier Optics*, McGraw-Hill: New York, Chapter 5, 96.